Cobalt Oxide Nanoparticles: Synthesis and Their Adsorption Study

Bahga Saleh[1], Samreen Fatema[1], Mazhar Farooqui[1], Shaikh Yusuf[2]

[1](Maulana Azad College of Arts, Science and Commerce, Aurangabad (MS), India)
[2](Shivaji College, Kannad (MS), India)
[2]Corresponding Author: shaikhyh@gmail.com

Abstract: *Nanoparticles are novel material because of their small size properties which is differ from its bulk material.This work aimed to study cobalt nanoparticles (Co-NPs) preparation using five different sol gel methods in order to evaluate the effect of synthesis variables that can influence the nanoparticles size distribution and particle shape. The synthesised nanoparticles were characterised by FTIR, SEM-EDX, and XRD. Out of these method five is more suitable and gives more accurate and appropriate results. The investigation process is carried out an adsorption study of all five NPs by different parameters such as effect of concentration of adsorbent, effect of concentration of dye, affect of pH, effect of contact time etc. were studied the adsorption capacity and adsorption behaviour of nanoparticals under various conditions. The experimental isotherm data has been studied. The kinetic study of the adsorption obeys Pseudo-first order model. The thermodynamic parameters namely Gibbs free energy, enthalpy, and entropy have revealed that the adsorption of methyl orange on the nanoparticlas is feasible, spontaneous and exothermic.*
Key Word: Sol-gel method, Nanoparticals, adsorption, FTIR ,SEM-EDX; XRD
_____

I.   Introduction

Nanostructured materials have been extensively investigated for the basic scientific. Sciences and Technological interests of access to new classes of functional materials with unprecedented properties and applications [1]. Nanoparticles are novel material because of their small size properties differ from those of their bulk counterparts [2].

The increasing interest in metal oxide nanoparticles relies on their outstanding properties in different fields like chemistry, optics, magnetism, electricity which in turn have produced current exploitation and application in catalysis, electronics, coatings and biomedical [3].

The transition metal oxide has greatly attracted a wide range of application in durable solar absorber, glucose sensor, lithium-ion batteries as electrode material, supercapacitors, and gas sensor [4]. Among the transition metal groups, Cobalt oxides have attracted much attention for their interesting fundamental properties and many technical applications. Co forms two stable oxides, CoO and Co3O4. The most stable form of CoO has a rock-salt structure and is antiferromagnetic below 289K [5]. The synthesis of pure CoO nanoparticles (NPs) is somehow difficult because of the greater thermodynamic stability of Co3O4 and the immediate reducibility of CoO to Co metal [6]. Co3O4 belongs to the normal spinel structure,which is based on a cubic close packing array of oxide ions in which Co(II) ions occupy the tetrahedral 8a sites and Co(III) ions ocuppy the octahedral 16d sites [7]. It is naturally abundant and environmentally safe besides excellent redox activity and low cost compared to other transition metal oxides, such as ruthenium. cobalt oxide exhibits good electrochemical performance in alkaline solution, Particularly as electrodes, in Co3O4 (cobaltosic oxide) form [8].

Cobalt oxide is an significant p-type semiconductor with direct optical band gaps at 1.48 and 2.19 eV [9]. Cobalt oxide, and cobalt-containing spinel oxides in particular, are subjects of enhanced interest as versatile electrocatalytic materials [10].

It is a metal oxide material with various industrial applications such as thin film catalysis, electro-chemical capacitor, heterogeneous catalysis, energy storage systems, solar cell, memory devices, Li – ion battery, gas sensor, magnetic materials, humidity sensors [11-14] .

Cobalt nanoparticles (Co-NPs) can be used to obtain catalysts for the Fischer–Tropsch synthesis (FTS) [15, 16]. Many sophisticated chemical processes, such as the sol–gel process, electrostatic spray decomposition, hydrothermal, co precipitation, water-in-oil emulsion method, electrostatic spray deposition, etc. have been developed to prepare highly active materials of high purity and crystallinity [17]. Sol-gel method is widely used among processing routes, due to its decisive advantages such as homogeneous mixing, good stoichiometric control, low synthesis temperature, fast heating time, and uniform particle size [18]. it is considered as the most effective one producing mesoporous structures and fine particles [19].

Now a day there are more than 10,000 dyes existing commercially the majority of which are thorny to biodegrade owing to their complex aromatic molecular structure and synthetic origin. Some dyes or their metabolites are either poisonous or mutagenic and carcinogenic unfavorable effect of dyes on environment and human such as skin, lung and other respiratory disorders are also accounted [20]. Several synthetic dyes including cationic (basic dyes), anionic dyes (direct, acid and reactive dyes) and non ionic dyes (disperse dyes and vat dyes) [21].

Dye molecules consists of two main components: the chromophores, which are largely responsible for colour production and the auxo-chromes, which are not only complement the chromophore but also make the molecule soluble in water and improve its affinity (attachment) toward the fibers[22]. The removal of dyes in an economic way remains an important issue for researchers and environmentalists [23]. Many treatment methods are available to remove dyes, which can be divided into physical, chemical, and biological methods [24].

Biological methods have the advantage of low cost, it takes long duration time to proceed Chemical methods and Filtration method exhibits heavy sludge to dispose with hazadorous contaminates [25]. Chemical methods which include (oxidation, reduction, and electrochemical), biological methods which include (aerobic and anaerobic degradation), physical methods which include adsorption, ion exchange, and membrane filtration are effective for removing reactive dyes without producing unwanted by-products. These include physicochemical methods such as filtration, coagulation, use of activated carbon and chemical flocculation .These methods are effective but they are not cheap and involve the formation of a concentrated sludge that creates a secondary disposal problem which requires safe disposal [26, 27].

Among these technologies, adsorption is considered as a superior technique due to its high efficiency, economics of implementation, feasible, insensitive to toxic substances and simplicity of design . The effect of various variables such as contact time, pH, adsorbent dosage, effect of volume of dye solution [28-30]. MethyI orange (MO) dye is used as the coloring agent, disinfector in dyestuffs, rubbers, pharmaceuticals, pesticides, and varnishes [31].

In the present study, CoO nanoparticles has been synthesized by five different methods and characterized and used as adsorbent for adsorption study of methyI orange.

II. Material And Methods

In this study, CoO nanoparticles is prepared by Sol-Gel method by five different ways. All five NPs were characterized by FT-IR, SEM-EDX, XRD and subjected for the adsoption on Methyl orange by different parameter i.e change in time, change in concentration of dye, change in weight of adsorbent, change in pH. The variation is reprsented by graph. For the present work double distilled water is used , cobalt chloride , sodium hydroxide , potassium hydroxide, methanol , ethanol, oxalic acid , glacial acetic acid, and methyI orange were of AR grade from SD fine chemical Ltd India. The paid services of various labs were taken for FT-IR, SEM, EDX, XRD ect. Five methods were used for the preparartion of nanoparticles are as follow.

Method 1 (M1) for the synthesis of cobalt oxide nanoparticles, 2gm of cobalt chloride was dissolved in 500 ml distilled water and kept on stirring. In another beaker HCl (36.5% HCl in distilled water) was prepared and 20 ml ethanol was added to cobalt solution and refluxed at 700C for 2 hrs, pink precipitate was appeared. The resulting gel was centrifuge for 10 min at 2000 rpm and washes several time with deionisied water. The residue mass was dried in a hot air oven at 120oc. The resulting compound underwent calcination using muffle furnace at 4500 C for two hrs to give cobalt oxide nanoparticles [32].

Method 2 (M2) for the synthesis of cobalt oxide nanoparticles, 2gm of cobalt chloride was dissolved in 200 ml of methanol and kept on stirring. In another beaker a solution of 6 gm of oxalic acid was dissolved in 200 ml of methanol and added to above warm solution to yield a thick gel and stirrer at 35oC under constant stirring for 30 min. The resulting gel was centrifuge for 10 min at 2000 rpm and washes several time with deionisied water. The

residue mass was dried in a hot air oven at 120oc. The resulting compound underwent calcination using muffle furnace at 4500 C for two hrs to give cobalt oxide nanoparticles [33].

Method 3 (M3) for the synthesis of cobalt oxide nanoparticles was carried out by taking 9 gm of cobalt chloride and 5.4 gm of sodium hydroxide pellet were dissolved in 200 ml of methanol separately. The amount of methanol used was as minimum as required. Methanolic solution of cobalt chloride was kept on magnetic stirrer. Sodium hydroxide solution was added drop by drop with continuous stirring at room temperature for 3 hrs. The colour of the solution was turned to pink. The resulting gel was centrifuge for 10 min at 2000 rpm and washes several time with deionisied water. The residue mass was dried in a hot air oven at 120oc. The resulting compound underwent calcination using muffle furnace at 4500 C for two hrs to give cobalt oxide nanoparticles [34].

Method4 (M4) for the synthesis of cobalt oxide nanoparticles, 2gm cobalt chloride was dissolved in 500 ml distilled water. This solution was kept on stirring. To this stirr solution 1 ml of glacial acetic acid was added. The solution was heated at 100oC for 30 min. Drop wise addition aqueous of sodium hydroxide 8 M was carried out with continuous stirring. Till the colour of solution turned to pink. The resulting gel was centrifuge for 10 min at 2000 rpm and washes several time with deionisied water. The residue mass was dried in a hot air oven at 120oc. The resulting compound underwent calcination using muffle furnace at 4500 C for two hrs to give cobalt oxide nanoparticles [35].

Method 5 (M5) for the synthesis of cobalt oxide nanoparticles was carried out by taking 2 gm of cobalt chloride and 8M of KOH were dissolved in benzene and hexane mixture (1:1 ratio) separately. Solution of cobalt chloride was kept on magnetic stirrer. KOH solution was added drop by drop with continuous stirring. The solution was stirred and refluxed for 2 hrs. The resulting gel was centrifuge for 10 min at 2000 rpm and washes several time with deionisied water. The residue mass was dried in a hot air oven at 120oc. The resulting compound underwent calcination using muffle furnace at 4500 C for two hrs to give cobalt oxide nanoparticles [36].

The nanoparticles so formed were subjected to FT-IR, SEM, EDX and XRD analysis.

The adsorption study was carried out using batch adsorption method. The effect of initial concentration of dye, PH, dosage form, contacts time etc was carried out as desorbed in earlier work. The nanoparticles were washed several times with distilled water till it becomes free from NaCl. Methyl orange (MO) determined by using UV-visible spectrophotometer (S2-159) at λmax = 470 nm. The adsorption experiment were carried out in stirred batch mode .For experiment, 10 ml of MO dye solution of specified concentration was continuously stirred unit 0.1 gm of powder at room temperature.

III. Result and Discussion

Fourier Transform Infrared Spectroscopy (FTIR) analysis: The FTIR spectrum of CoO within the wave number varies from 4000 - 400 cm-1 as shown in Fig.1shows FTIR spectra of CoO nanoparticles synthesized by sol-gel technique. FTIR Spectroscopy was carried out in order to ascertain the purity and nature of metal or metal oxide nanoparticles. The FTIR for all five types of nanoparticles has same common peaks, also alongwith same different spectral peaks. The absorption band at 536.114 cm-1, 570.826cm-1 was assigned to Co-O stretching vibration mode and 663.393cm-1 was assigned to the bridging vibration of O-Co-O bond. The low energy region and large broad band at 624.823 cm-1 indicates the stretching mode of Co-O bond of a CoO network. Additionally, two more distinct peaks at 686.534 cm-1 and 717.39 cm-1 are indicative of the presence of optical vibration modes of cobalt oxide [37]. The band at 466.689 cm-1, 667.25cm-1 and 509.115 cm-1 were found that corresponds to the metal-oxygen (Co-O) stretching vibration modes of CoO bond. Metal oxides are generally found to give absorption bands below 1,000 cm-1 that arise due to interatomic vibration [38]. Two absorption bands centered at 628.68 cm-1 and 547.685 cm-1 are assigned to the fingerprint stretching vibrations of Co-O bond [39]. The band at 565 cm-1 is related to Co-O vibrations in the octahedral site; whereas the band at 651 cm-1 is associated to Co-O vibrations in the tetrahedral site of the lattice, indicating the formation of pure phase of CoO. The presence of these bands in the lower wave number region suggests that the materials were finely crystallized in the nano range [40].
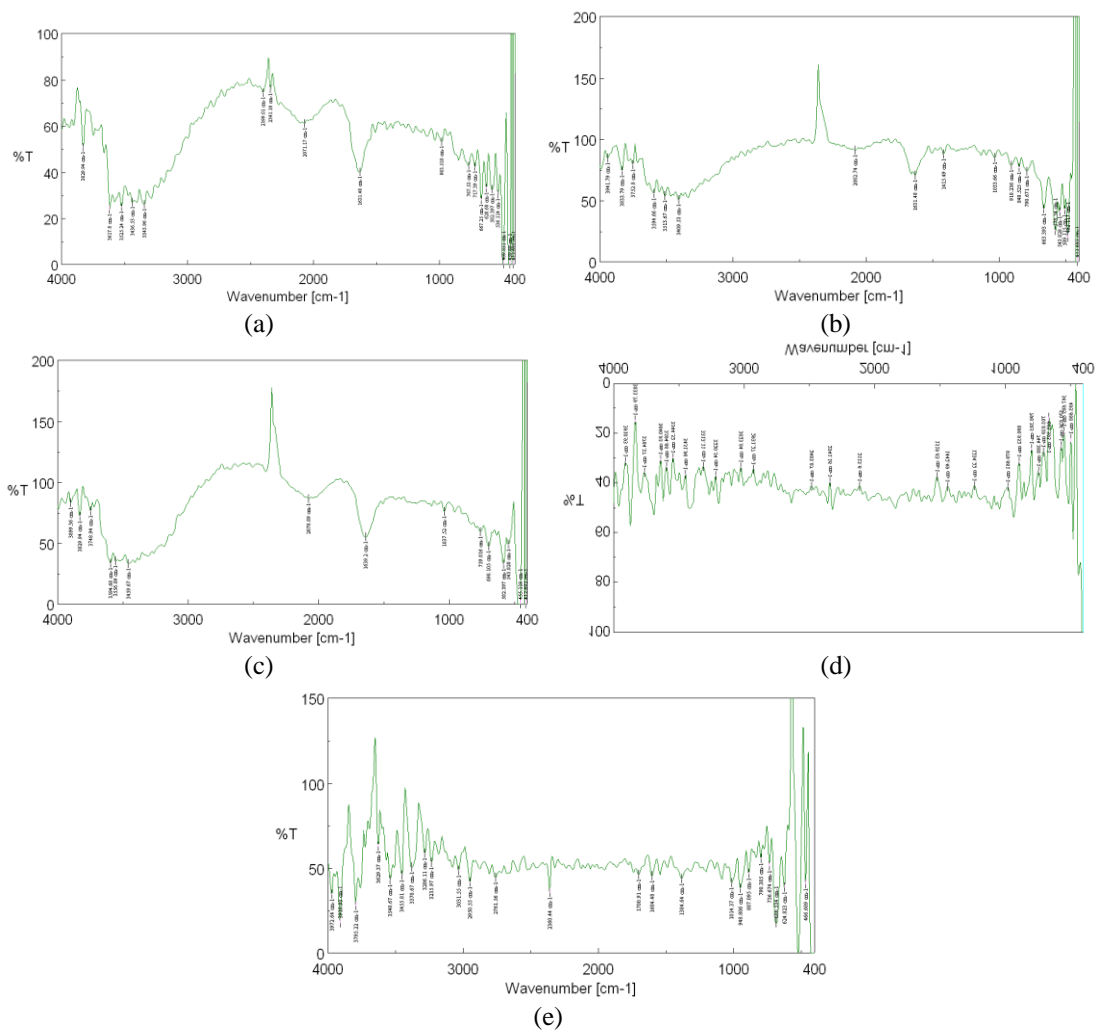
(a)

(b)

(c)

(d)

(e)

Figure no 1: FTIR of CoO Nanoparticles synthesized by
(a) Method 1 (b) Method 2 (c) Method 3 (d) Method 4 (e) Method 5

Scanning Electron Microscopy (SEM-EDX): The surface morphology of the as prepared cobalt oxide nanoparticles was carried out by using Scanning Electron Microscope (SEM). The SEM micrograph of the CoO calcined at 450°C. Fig.2 shows the SEM image of the nanoparticle which clearly indicates that the nanoparticles are homogeneous and agglomerated. It can be seen from the image that the particle size is in the range of nanometer having irregular morphology with different sized particle 12.9, 23.6, 16.3, 33.2 and 26.4(nm). To check the chemical composition of synthesized CoO nanoparticles was measured by Electron Diffraction X-ray Analysis .The spectrum shows the strong X-ray peaks associated with Co and O elements in CoO in nanoparticles and other peaks are also obtained in EDAX which may be due to the chemicals which were added during processing of nanoparticles were found in the EDAX spectrum as shown in Fig.3 Cobalt oxide nanoparticles synthesized by five procedures in which M4 gives more amounts of cobalt oxide nanoparticles is 25.38 0.04, while M1 gives least amount of nanoparticles that is10.07±0.05. Table 1. shows the percentage of all elements present in the nano powder.
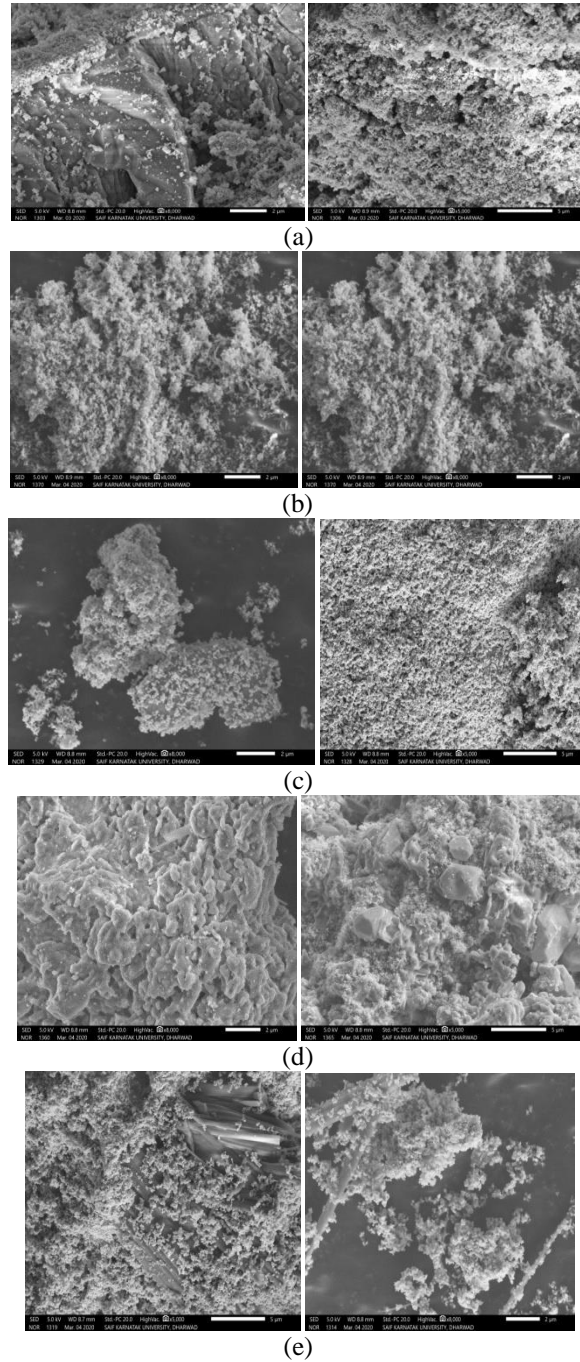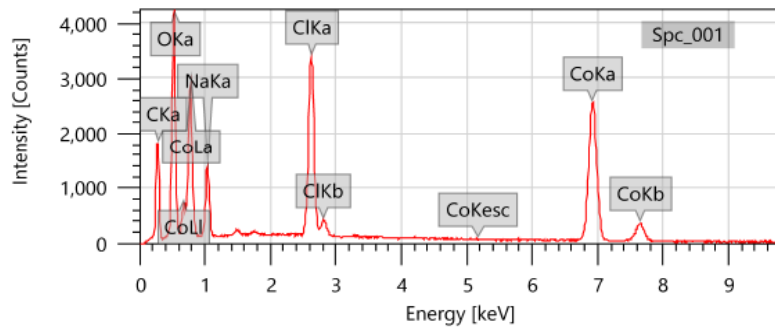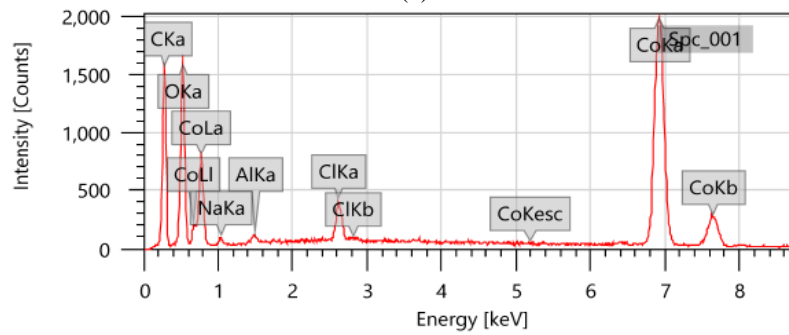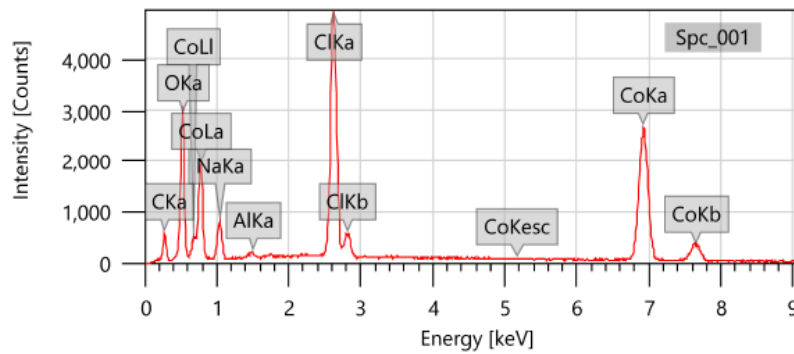
Figure no 2: SEM images of CoO Nanoparticles
(a) Method 1 (b) Method 2 (c) Method 3 (d) Method 4 (e) Method 5
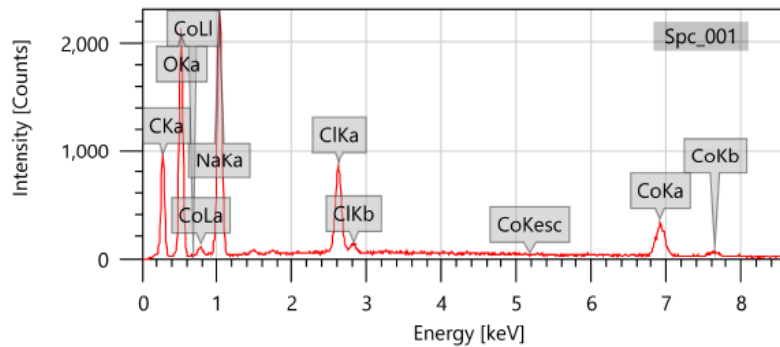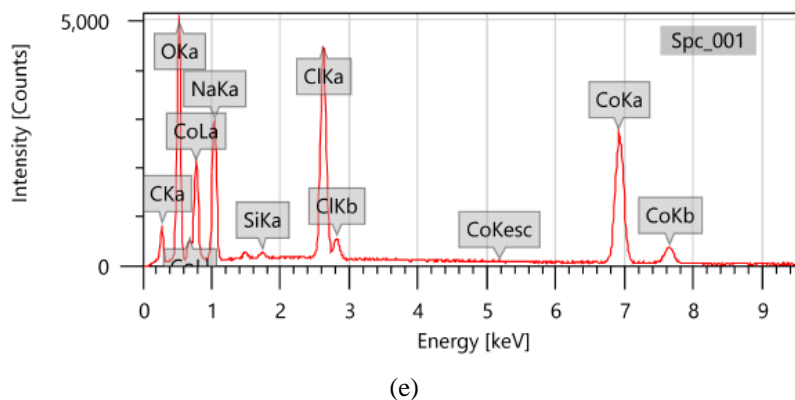
(a)

(b)

(c)

(d)

(e)

Figure no 3: EDAX of CoO Nanoparticles
(a) Method 1 (b) Method 2 (c) Method 3 (d) Method 4 (e) Method 5

Table no 1: percentage of all elements present in the nano powder

Element	M1	M2	M3	M4	M5
C	43.09±o.18	32.15±0.24	30.78±0.23	41.64±0.24	26.32±0.17
O	37.53±0.19	28.98±0.23	37.93±0.23	40.07±0.28	42.62±0.19
Na	4.96±0.06	0.54±0.04	4.80±0.07	13.70±0.11	12.52±0.09
C 1	4.35±0.03	0.90±0.02	10.08±0.05	2.20±0.03	6.70±0.03
Co	10.07±0.05	16.20±0.10	16.08±0.08	25.38±0.04	21.67±0.06

X-ray diffraction analysis (XRD): Fig.4 the typical X-ray diffraction (XRD) spectrum of cobalt oxide (CoO) nanoparticles is shown in Figure. The intensity peaks and scattering angle of synthesized (CoO) nanoparticles is well consistent with cobalt oxide.

M1 was recorded in the fraction angle range 5° to 55°. The peak appears at 31.47º, 36.64º and 45.26º are observed, corresponding to the (210), (301) and (222) planes of CoO crystals. The highest peak is at angle 31.47° at (210) plane with 483.71 intensity.

M2 was recorded in the fraction angle range 5° to 35°. The peak appears at 9.25°, 19.1°, 23.27°, 28.41°, 29.93° and 31.27° are observed, corresponding to the (100), (200), (202), (300), (004) and (104) planes of CoO crystals. The highest peak is at angle 31.27° at (110) plane with 3807.93 intensity.

M3 was recorded in the fraction angle range 5° to 20°. The peak appears at 6.04°, 8.44°, 9.42°, 10.23°, 10.84° ,12.2º, 13.87º, 14.47º, 15.86º and 16.57° are observed, corresponding to the (100), (002), (110), (102), (111), (201) ,(103), (202), (211) and (113) planes of CoO crystals. The highest peak is at angle 9.42° at (110) plane with 292.91intensity.
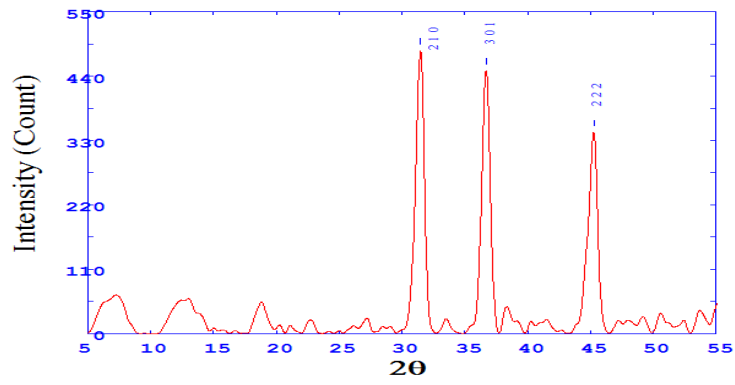
M4 was recorded in the fraction angle range 5° to 20°. The peak appears at 11.45°, 12.78° and 16.42° are observed, corresponding to the (002), (110) and (201) planes of CoO crystals. The highest peak is at angle 11.45° at (002) plane with 4342.87 intensity.

M5 was recorded in the fraction angle range 5° to 25°. The peak appears at 6.39°, 7.41°, 8.18°, 10.02°, 11.14°, 12.28º, 13.26º, 14.07º, 15.33º , 17.07º, 18.22º, 19.11º, 20.32º and 21.36º are observed, corresponding to the (100), (101), (002), (110), (200), (201) ,(112), (202), (210) ,(300), (004), (302), (221) and (204) planes of CoO crystals. The highest peak is at angle 19.11° at (302) plane with 301.76 intensity.
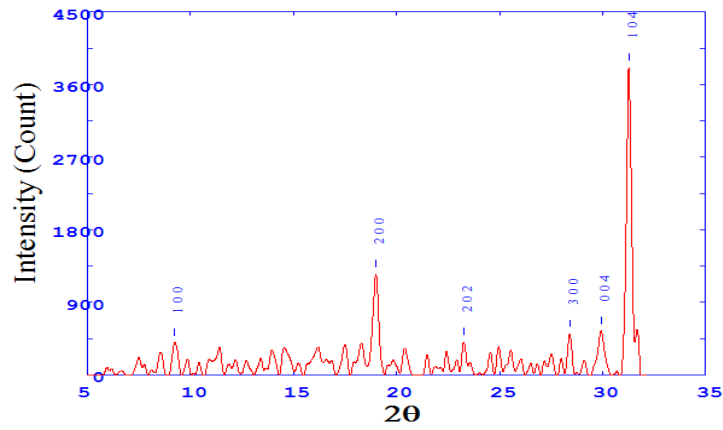
Particle size of the investigated CoO-NPs was calculated from line broadening analysis of some diffraction line of metal oxide phase using Sherrer equation. The inspection of these figure revealed that the CoO-NPs prepared by these methods and calcined at 450°C consist of crystalline CoO phase which quality of crystallinity increases by increases of calcination temperature. The CoO nanoparticles prepared from these methods and calcined at 450o c have crystalline average size 10.7, 29.2, 22.5, 8.6, 22.9 (nm) respectively which calculated from XRD pattern and Scherrer equation.
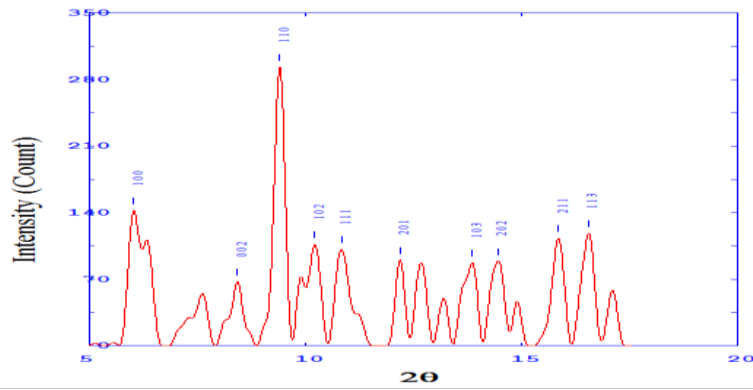
$$D = K\lambda / \beta \cos\theta$$

where, K = 0.89 is the shape factor, λ is the x-ray wavelength, B is the line broadening at half the maximum intensity (FWHM) in radians, and θ is the Bragg angle.
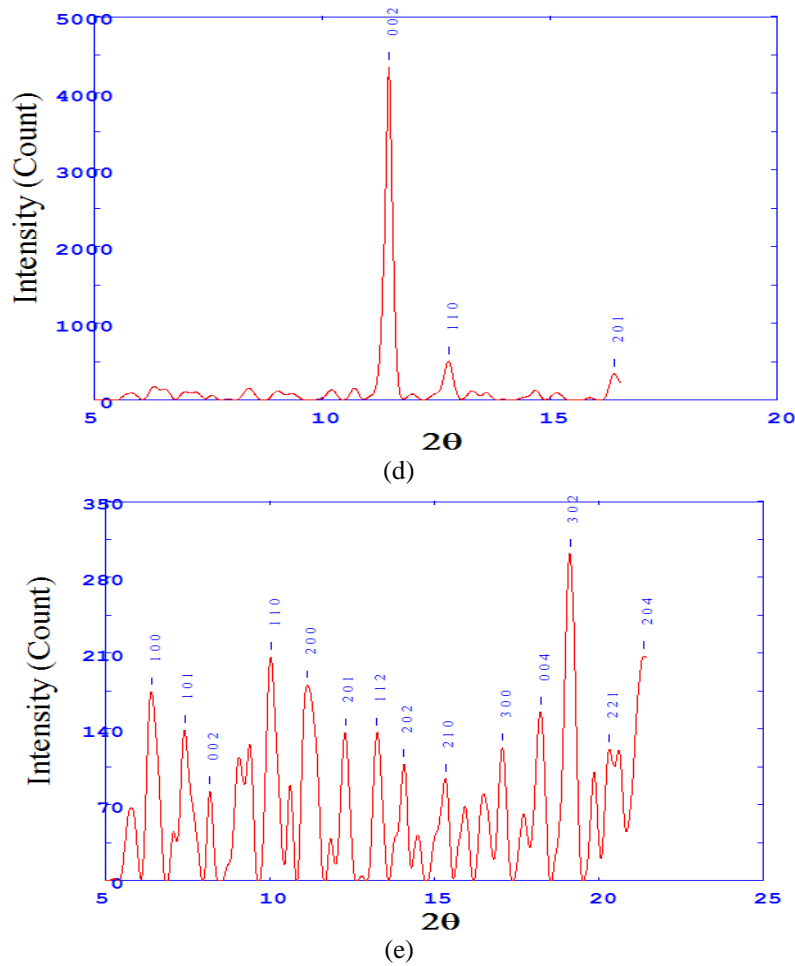
(a)

(b)

(c)

(d)

(e)

Figure no 4: XRD of CoO Nanoparticles
(a) Method 1 (b) Method 2 (c) Method 3 (d) Method 4 (e) Method 5

The IR and XRD confirm the confirmation of CoO nanoparticles. These nanoparticles are used for the evaluation of their adsorption capacities. The SEM images proves that the surface of particles is rough and can adsorb the dye. For present study, Methyl Orange (MO) is used as adsorbate.

Adsorption study: Effect of contact time: In adsorption studies, effect of contact time plays vital role irrespective of other experimental parameters effecting adsorption kinetics. The sample of dye was taken in separate flasks and adsorption studies were carried out at different contact time from 5 – 25 min. The results are given in Fig.5.
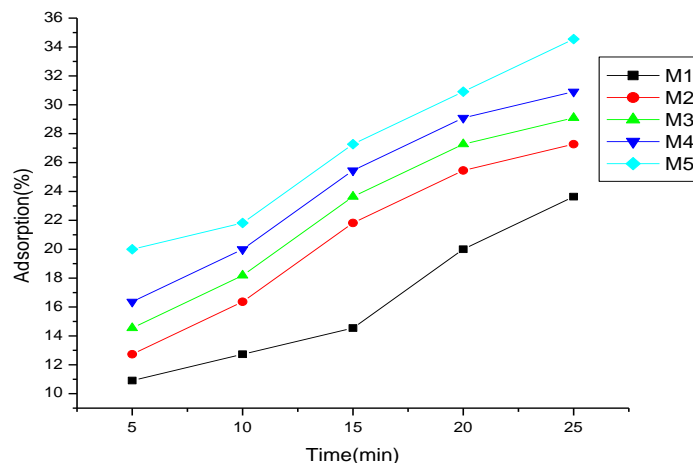
Figure no 5: Effect of contact time

It is observed that adsorption increased with increased in time of contact as shown in Fig.5 it is indicated that the adsorption increased with time of contact until equilibrium was reached. This means that as adsorption starts, there are active sites available which got occupied and coordinatively consumed with increased time there by clogging. The sorption sites and a reduction or un availability of free sites.

Effect of dosage: At room temperature with an initial concentration of 100mg/L, 10 mL of MO dye solution was added to 5 beakers, then the dosage of adsorbent was introduced in the beakers as 0.1, 0.2, 0.3, 0.4 and 0.5 g, respectively, and the adsorption time was set for 10 min.
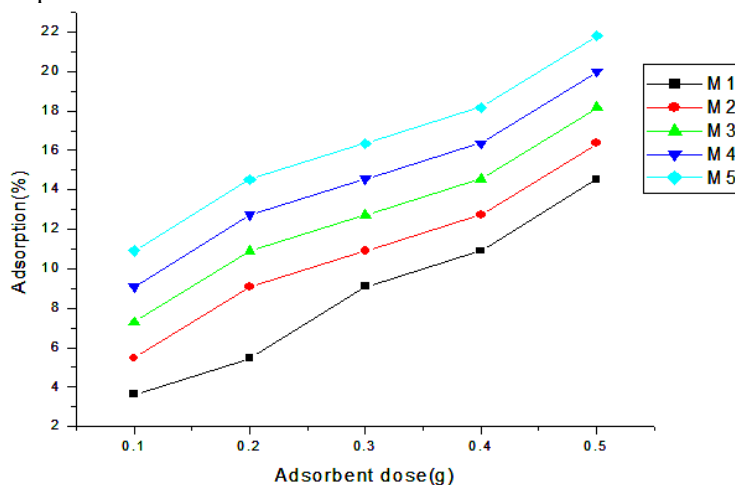

Figure no 6: Effect of adsorbent

The effect of adsorbent dosage on the percentage removal of MO dye is shown in Fig.6 it is observed that the percentage removal of MO dye from solution increased with increasing adsorbent dosage. This increase in the percentage removal can be attributed to the increased surface area of the adsorbent and availability of more adsorption sites. The maximum dye removed efficiency has been achieved at 0.5g of the sorbent.

Effect of initial concentration: At room temperature with an initial concentration of 2, 4, 6, 8 and 10 mg/L, 10 mL of MO dye solution was added to 5 beakers, then 0.1g of adsorbent was added to each beakers, and the adsorption time was set for 10 min.

The effect of initial concentration on the percentage removal of MO dye is shown in Fig.7 the percentage of adsorption is increases by increase in adsorption dose. The increase in adsorption with increase in adsorbent dosage may be due to the increase in availability of the active sites, because of the increase in the active surface area of the adsorbent.

Figure no 7: Effect of initial concentration

     The effect of initial concentration on the percentage removal of MO dye is shown in Fig.7 the percentage of adsorption is increases by increase in adsorption dose. The increase in adsorption with increase in adsorbent dosage may be due to the increase in availability of the active sites, because of the increase in the active surface area of the adsorbent.
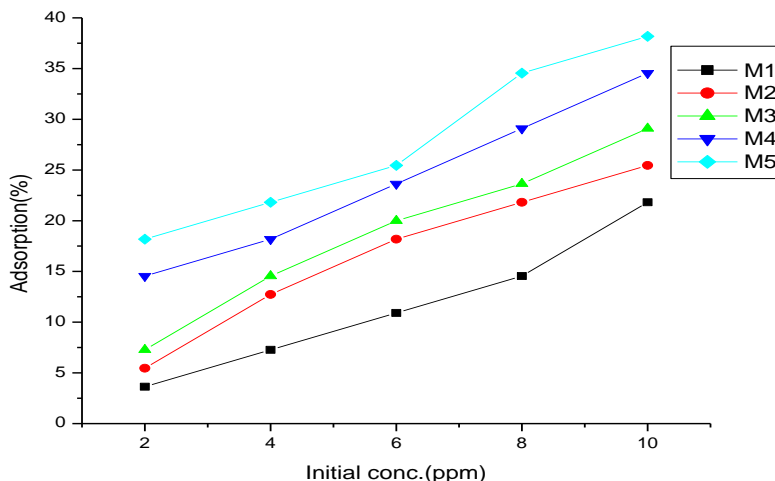
Effect of PH: At room temperature with an initial concentration of 100mg/L, 10 mL of MO dye solution was added to 5 beakers, then 0.1g of adsorbent was added to each beakers ;however ,the PH of MO dye solution in the 5 beakers was adjusted by hydrochloric and acid and sodium hydroxide solution to be 2,4,6,8,10,respectively,and the adsorption time was set for 10 min.
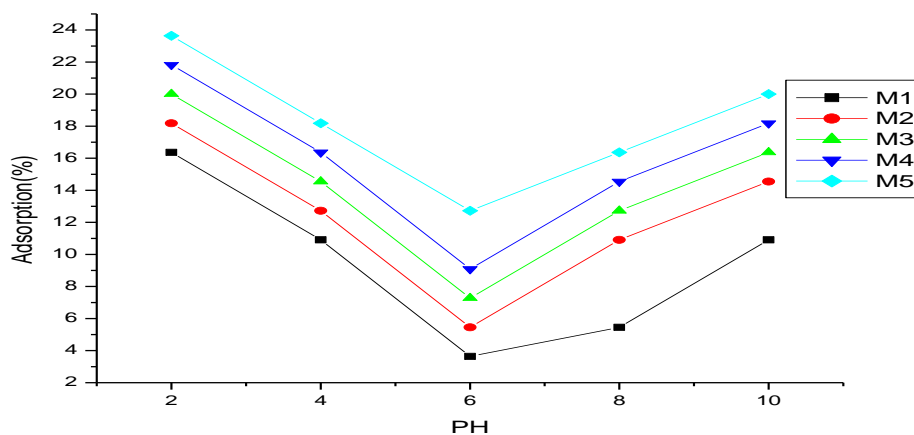

Figure no 8: Effect of pH

     The result has been obtained are shown in Fig.8 which described the maximum adsorption at PH= 2 i.e. acidic pH. And there after the adsorption decreases till pH = 6. In basic pH adsorption get increases.

Effect of temperature: The equilibrium percentage removal of MO dye onto CoO-NPs was studies by varying the temperature from 298 K to 232 K. The experiments were performed by adding 0.1 g of CoO-NPs into 10 mL of 100 ppm solutions of MO dye Fig. 9.

     The obtained results showed that the increase in the temperature of the solutions of MO dye from 298 K to 232 K leads to an increase in the adsorption percentage removal of CoO-NPs. The possible explanation of this increase in percentage removal of MO dye onto CoO-NPs could be due to the availability of more active sites and activation of the adsorbent surface at higher temperatures. It could also be due to the increased diffusion and mobility of MO dye ions from the bulk solution toward the CoO-NPs surface, there by increasing the number of dye molecules acquiring sufficient energy to undergo chemical reaction with CoO-NPs at higher temperature.
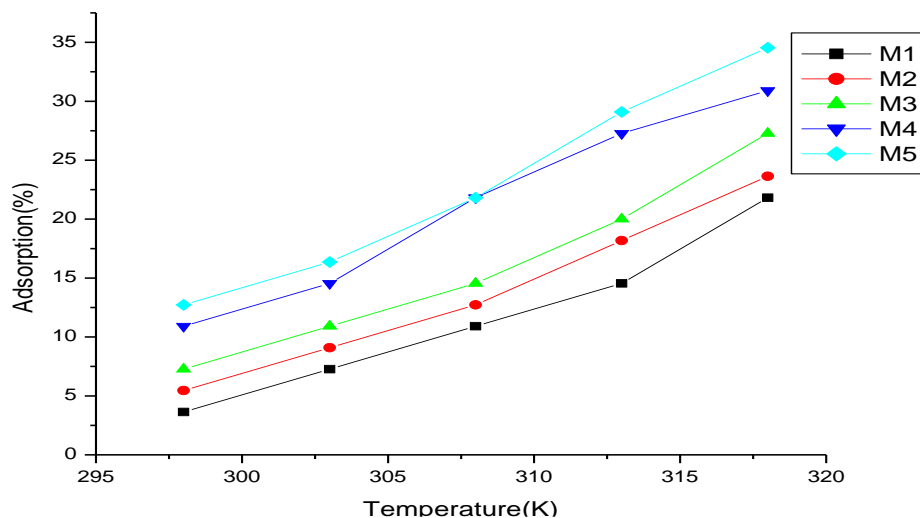
Figure no 9: Effect of temperature

Adsorption isotherm: Kinetic isotherm: In the present work, Pseudo first order and Pseudo second order kinetic models can be expressed in a linear form as the following equations:

$$Ln(Qt - Qe) = LnQe + K1t \qquad (1)$$

$$\frac{t}{Qt} = \frac{1}{K2Q2e} + \frac{t}{Qe} \qquad (2)$$

Where q_e and q_t are the amount of MO adsorbed at equilibrium and different time (min) respectively K1 represents the first order constant (min-1) [41].

Table no 2: Comparison of the experiments and the kinetic model of MO dye on CoO Nanoparticles adsorbet

Method	Conc. Of MR (mg/L)	Pseudo-First order			Second order		
		K1 (min-1)	qe (mg/gm)	R2	K2 (gm/mg.min)	qe (mg/gm)	R2
M1	10	0.086737	7420.446	0.944881	1.8x10-5	3538.558	0.784057
M2	10	-0.09765	7692.721	0.986674	2.59x10-5	4187.482	0.978477
M3	10	-0.10052	7513.287	0.980793	1.92x10-5	4090.917	0.967312
M4	10	-0.11756	6618.354	0.981546	2.27x10-5	4116.632	0.973833
M5	10	-0.11278	6920.222	0.982933	2.79x10-5	4401.215	0.955624

To understand the nature of the interaction between the adsorbent and the methyl orange dye, the linearized forms of the Langmuir and Freundlich isotherms are used to analyze the experimental data obtained.
The linearized form of the Langmuir isotherm equation is as show in equation below:

$$\frac{1}{qe} = \frac{1}{qm} + \frac{1}{KLqmCe} \qquad (3)$$

Where Ce is the equilibrium concentration of the MO, qe is MO amount adsorbed at equilibrium qm and KL are Langmuir constants related to the adsorption capacity and adsorption energy, which can be calculated from linear regression 1/qe vs 1/ce [42].

The shape of this isotherm can also be expressed in terms of separation factor (RL), which is given as follows:

$$R_L = \frac{1}{1-bC0} \qquad (4)$$

Where Co (mg/L) is the initial in liquid phase. The values of RL indicates the adsorption isotherm model of characteristic as follows RL>1 (unfavorable), RL=1 (Linear), 0 < RL < 1 (favorable) and RL= 0 (irreversible).

The Freundlich model is based on the sorption onto a heterogeneous surface. The linear expression of Freundlich equation is as follow:

$$\ln q_e = \ln K_f + \frac{1}{n}\ln C_e \tag{5}$$

Where KF and n are the Freundlich constants, being indicators of adsorption capacity and adsorption intensity, respectively. Log qe at different temperatures versus log Ce [43].

Table no 3: Adsorption constant

Method	Conc. Of MO (mg/L)	Langmuir constant				Freundlich constant		
		Q0 (mg/gm)	b*10-5 (L/gm)	RL	R2	n	Kf (mg/gm.(L/gm))1/n	R2
M1	10	-0.36376	-0.0104	-25.3119	0.423033	0.133857	2.67x10-13	0.8009
M2	10	-588.235	-6.4x10-6	1.000643	0.812738	0.21787	4.43x10-8	0.827099
M3	10	2.499313	0.039842	0.200634	0.99986	0.169126	1.57x10-10	0.857939
M4	10	-507.614	-1.36806	-0.00736	0.8836	0.147771	4.6x10-12	0.871777
M5	10	-526.316	-0.01013	-77.5124	0.898704	0.13626	4.8x10-13	0.880369

Thermodynamic parameter

Thermodynamic parameters were determined using equation:

$$\Delta G^o = \Delta H^o - T\Delta S^o \tag{6}$$

$$\text{Log}\left(\frac{qe}{ce}\right) = \frac{\Delta So}{2.303R} + \frac{-\Delta Ho}{2.303RT} \tag{7}$$

Where qe is the amount of MO adsorbed per unit mass of NPs(mg / g) and ce is the equilibrium concentration(mg / L). The log(qe / ce) vs $\frac{1}{T}$ gives the values of ΔS^o and $-\Delta H^o$ as intercept and slope.Hence ΔG^o can be calculated.

Table no 4: Thermodynamic parameter values

Sr. No.	Temp (K)	ΔG_0(M1)	ΔG_0(M2)	ΔG_0(M3)	ΔG_0(M4)	ΔG_0(M5)
1.	298	5203.989	4770.906	4387.842	4042.681	3435.263
2.	303	4850.955	4110.511	3789.667	3492.902	3215.744
3.	308	4535.085	3268.809	3003.54	2752.019	2512.074
4.	313	3608.179	2796.694	2552.854	2318.981	2093.582
5.	318	3101.057	2593.635	2356.025	2127.026	1689.937

Table no 5: values of enthalpy and entropy

Sr. No.	Method	ΔS^o	ΔH^o
1.	M1	108.3688	-37637.5
2.	M2	114.1926	-38679.4
3.	M3	106.7398	-36093.7
4.	M4	100.7611	-33981.1
5.	M5	92.19272	-30984.7

IV. Conclusion

In the summary of present work, CoO nanoparticles were successfully achieved by sol gel method. All methods are good for the preparation of nanoparticals but forth method is more appropriate and gives more amount of cobalt oxide nanopartical. The FTIR spectra of forth method give more relevant bands and SEM image shows the crystal structure. EDX data shows all methods are not free from NaCl . Further it is revealed the NPs prepared by the forth method is the most efficient adsorbent for MO and it confirms that the adsorption depends on various factors includes method of preparation.

References

[1]. Manigandan R, Giribabu K, Suresh R, Vijayalakshmi L, Stephen A and Narayanan V.(2013). Cobalt Oxide Nanoparticles: Characterization and its Electrocatalytic Activity towards Nitrobenzene. J. of Chem Sci Trans, 2(1), 47-50.

[2]. Jagtap S, Tale A, Thakre S.(2017). Synthesis By Sol Gel Method And Characterization Of Co3O4 Nanoparticles. J. of R in Eng and Appl Sci (IJREAS), 7 (8), 1-6.

[3]. Igor Luisetto AE Franco Pepe AE Edoardo Bemporad.(2008). Preparation and characterization of nano cobalt oxide. J.of Nanopart Res,10, 59–67.

[4]. Wadekar K, Nemade K and Waghuley A.(2017). Chemical synthesis of cobalt oxide (Co3O4) nanoparticles using Co precipitation method. R J of Chem sci,7(1), 53-55.

[5]. Ulrika L, Mikael O, Annika P.(2014). Synthesis and characterization of cobalt oxide and composite thin films. Adv in Mater, 3(5), 52-57.

[6]. Subrata K, Jayachandran M.(2013). Shape-selective synthesis of non-micellar cobalt oxide (CoO) nanomaterials by microwave irradiations. J Nanopart Res,15(1543), 2-13.

[7]. Ana O, America V, Roberto S and Roberto E. (2009).Hydrothermal Synthesis of Co3O4 Nanooctahedra and Their Magnetic Properties. Rev.Adv.Mater.Sci, 22, 60-66.

[8]. Michele K , Carlos S , Querem H, Rodrigo F, Raimundo R, Edgardo f, Leandro A.(2018). Pseudocapacitance Properties of Co3O4 Nanoparticles Synthesized Using a Modified Sol-Gel Method. Мater R, 0521,1980 - 5373.

[9]. Vikas P, Pradeep J, Manik C, Shashwati S. (2012).Synthesis and Characterization of Co3O4 Thin Film. Soft Nanoscience Letters, 2, 1-7.

[10]. Naoufal B, Peter A, Janine F, and Katharina K.(2007). Preparation of Doped Spinel Cobalt Oxide Thin Films and Evaluation of their Thermal Stability. Chem. Vap. Deposition, 13, 118–122.

[11]. Sinduja C, Kalpanadevi K, Manimekalai R.(2013). Characterization of Nanostructured Cobalt Oxide Particles Synthesized By Thermal Treatment.Global R analysis, 2(7),11-13.

[12]. Anjali A, Megha M, Hema S and Navinkiran K. (2010), Synthesis of Cobalt Oxide Nanoparticles/Fibres in Alcoholic Medium using g-ray Technique. Def Sci J, 60(5), 507-513.

[13]. Manimekalai R, Thrivikraman K and Sinduja C. (2012). Synthesis of Cobalt Oxide Nano Particles from Hydrazine Metal Carboxylate Complexes. I J of Chem and Appli,4(2), 97-102.

[14]. Sharifi S, Shakur H, Mirzaei A, Salmani A, Hosseini M. (2013). Characterization of Cobalt Oxide Co3O4 Nanoparticles Prepared by Various Methods: Effect of Calcination Temperatures on Size, Dimension and Catalytic Decomposition of Hydrogen Peroxide. Int. J. Nanosci. Nanotechnol, 9(1), 51-58.

[15]. Andre Z, Renata R, Jose B, Daniela Z and Pedro A. (2014). Cobalt nanoparticles prepared by three different methods. J of Exp Nanoscience, 9(4), 398- 405.

[16]. Madeleine D, Ola N, Helmer F.(2011). Thin Films of Cobalt Oxide Deposited on High Aspect Ratio Supports by Atomic Layer Deposition. Chem. Vap. Deposition, 17, 135–140.

[17]. Ramdas B, Amit C, Kulkarni B, Gopukumar S, Sivashanmugam A.(2008). Preparation and electrochemical characterization of lithium cobalt oxide nanoparticles by modified sol–gel method. Mater R Bull, 43, 2497–2503.

[18]. Sina S and Sirous A.(2010). Characterization of LiCo Nanopowders Produced by Sol-Gel Processing. J of Nanomaterials, ID 104012, 1-8.

[19]. Gomaa A, Osama A and Salah A. (2016). Electrical Properties of Cobalt Oxide/Silica Nanocomposites Obtained by Sol-Gel Technique. Ameri J of Eng and Appl Sci, 9(1), 12-16.

[20]. Ameeth B, Nagalakshmi R.(2016). Shanthi. Removal of congo red and magenta dyes from industrial waste water by thorn apple leaf powder. Int. J. Chem. Sci,14(1), 57-64.

[21]. Radwan N, Hagar M , Chaieb K.(2016). Adsorption of Crystal Violet Dye on Modified Bentonites. Asian J of Chem, 28(8), 1643-1647. : 2223-9944

[22]. Rajamani M and Xavier A.(2018). Adsorption of reactive magenta and methyl red from aqueous solution using. I J of Current R, 10(8), 72565-72574.

[23]. Deepak P, Shikha S, Pardeep S.(2017). Removal of methylene blue by adsorption onto activated carbon developed from Ficus carica bast. Arabian J of Chem, 10, 1445–1451.

[24]. Nirmala S, Pasupathy A, Raja M.(2016). Removal of Malachite Green from Aqueous Solutions by Adsorption Using Low Cost Adsorbent Andrographis PaniculataLeaves. I Jof Sci and R Publications, 6(9), 689-693.

[25]. Kavithayeni V, Geetha K, Akash S.(2019) . A Review on Dye Reduction Mechanism using Nano Adsorbents in Waste Water. I J of Recent Tech and Eng (IJRTE), 7(6S2), 332-339.

[26]. Subir C, Tapan K.(2016). Adsorption of Reactive Blue 4 (RB4) onto Rice Husk in Aqueous Solution. I J of Sci& Eng R, 7(3), 7-12.

[27]. Masoud R, Mohsen I, Somayyeh A, Mostafa F, Fattaneh J.(2014). . Removal, preconcentration and determination of methyl red in water samples using silica coated magnetic nanoparticles. J of Appl R in Water and Wastewater, 1, 6-12.

[28]. Shi-chuan Wu, Xia You, Cao Yang and Jian-hua Cheng.(2017). Adsorption behavior of methyl orange onto an aluminumbased metal organic framework. MIL-68(Al), Water Science &technology , 75(12), 2800-2810.

[29]. Roxana I, Marcela S, Cornelia P, Cosmin L.(2019). Single and simultaneous adsorption of methyl orange and phenol onto magnetic iron oxide/carbon nanocomposites. Arabian J of Chem, 12, 3704–3722.

[30]. Conrad K, Nnaemeka J, Enenebeaku E, Ikechukwu C.(2017). Adsorption and Equilibrium Studies on the Removal of Methyl Red From Aqueous Solution Using White Potato Peel Powder. I Letters of Chem, Phy and Astro, 72, 52-64.

[31]. Paul E.(2013). Adsorption of methyl red and methyl orange using different three bark powder. Acad R J, 4(1), 330-338.

[32]. Sanchez E, lapez T.(1995). Effect of the preparation method on the band gap of titania and platinum-titania sol-gel materials.j of Mat latt , 25, 271-275.

[33]. Parmvir S, Rishab J, Nirmal K, Kaushik S and Jayendra S.(2015). Synthesis of Manganese Oxide NPs Using Similar Process and DifferentPrecursors–A Comparative Study. Nanotech R J, 8(3), 419-427.

[34]. Ismat Z, Lutfun N,. Sarwaruddin C, Gafur M, Nuruzzaman K, Ruhul A.(2015). Preparation and Characterization of Copper Oxide NPs Synthesized via Chemical Precipitation Method. Open Access Library J, 2(3), 1-8.

[35]. Hadeel K, Kadhim A, Ahmed A. (1017). Synthesis of copper oxide NPs via sol-gel method. (IJREI),1(4), 43-45.

[36]. Sanjay S, Mahendra k, Arvind A and Sudhanshu K.(2013). Synthesis and Characterisation of Copper Oxide NPs. IOSR-JAP, 5(4), 61-65.

[37]. Shadrokh S, Farahmandjou M and Firozabadi T.(2016). Fabrication and Characterization of Nanoporous Co Oxide (Co3O4) Prepared by Simple Sol-gel Synthesis Phys. Chem. Res, 4(2), 153 - 160.

[38]. Bhatt A, Bhat D, Tai C, Santosh M.(2011). Microwaveassisted synthesis and magnetic studies of cobalt oxide nanoparticles. Mater Chem Phys, 125, 347–350.

[39]. Chandrappa K, Venkatesha T.(2012). Generation of Co3O4 microparticles by solution combustion method and its Zn-Co3O4 composite thin films for corrosion protection. J of Alloys and Compounds, 542, 68-77.

[40]. Pudukudy M, Yaakob Z, Narayanan B, Gopalakrishnan A, Tasirin S.(2013). Facile synthesis of bimodal mesoporous spinel Co3O4 nanomaterials and their structural properties. Superlattices and Microstructures, 64, 15-26.

[41]. Nhamo C, Edna C, Willis G.(2017). Synthesis, characterisation and methyl orange adsorption capacity of ferric oxide–biochar nano-composites derived from pulp and paper sludge. Appl Water Sci ,7, 2175–2186

[42]. Shidong Li, Ole T, Hon C, Nanji J and Ludger P. (2019). The Impact of Nanoparticle Adsorption on Transport and Wettability Alteration in Water-Wet Berea Sandstone: An Experimental Study. Frontiers in Physics,7, 1-12.

[43]. Soheila H, Marzieh T and Seyed J.(2015). Removal of crystal violet from water by magnetically modified activated carbon and nanomagnetic iron oxide, Removal of crystal violet from water by magnetically modified activated carbon and nanomagnetic iron oxide. J of Envi Health Sci & Eng, 13(8), 2-7.